NATIONAL ADVISORY COMMITTEE FOR AERONAUTICS

TECHNICAL NOTE 3238

REVIEW OF INFORMATION ON INDUCED FLOW OF A LIFTING ROTOR

By Alfred Gessow

Langley Aeronautical Laboratory
Langley Field, Va.

Washington
August 1954

lB

NATIONAL ADVISORY COMMITTEE FOR AERONAUTICS

TECHNICAL NOTE 3238

REVIEW OF INFORMATION ON INDUCED FLOW OF A LIFTING ROTOR

By Alfred Gessow

SUMMARY

A brief review of the available information relating to induced flow of a lifting rotor is presented. The available material is summarized in a table as to flight condition, type of information, source, and the reference papers in which the data can be found. Some representative aspects of some of the reference material are discussed.

INTRODUCTION

A knowledge of the inflow distribution through and about a lifting rotor is required in almost all fields of helicopter analysis. Precise, detailed information on the subject is meager, however, because of the rather formidable difficulties involved in measuring or calculating rotor downwash accurately. Fortunately, a superficial estimate of the inflow distribution has proven adequate for many types of helicopter analyses and a fair amount of general information, both theoretical and experimental, is available on the subject. In view of the stimulation of interest in rotor induced flow brought about by the current emphasis on loads, stability and control, and the expanded use of multirotor configurations, it is considered desirable to review such information.

SYMBOLS

C_T thrust coefficient, $\dfrac{T}{\pi R^2 \rho (\Omega R)^2}$

r radial distance to blade element, ft

R blade radius, ft

T rotor thrust, lb

v induced inflow velocity at rotor, always positive, fps

V true airspeed of helicopter along flight path, fps or mph

Z vertical distance from plane perpendicular to rotor shaft, positive upward, ft

α rotor angle of attack; angle between projection in plane of symmetry of axis of no feathering and line perpendicular to flight path, positive when axis is pointing rearward, radians

ϵ downwash angle induced by rotor, radians

μ tip-speed ratio, $\frac{V \cos \alpha}{\Omega R}$

ρ mass density of air, slugs/cu ft

Ω rotor angular velocity, radians/sec

Subscript:

HOV hovering

OUTLINE OF INFORMATION

The available material on rotor induced flow is summarized in table I as to flight condition, type of information, source, and the reference papers (see refs. 1 to 28) in which the data can be found. The flight conditions covered in the table are hovering, vertical ascent and descent, low-speed forward flight, and cruise and high-speed forward flight. A study of the information presented in the table shows that the inflow problem has been attacked theoretically, as well as by wind-tunnel tests on small- and large-scale models, by helicopter tower tests, and by flight tests on actual production helicopters. The experimental data consist of measurements of the magnitude and distribution of the rotor inflow, as well as flow-visualization data using smoke and balsa-dust techniques. It should be understood that both theory and experiment yield only time averages of the inflow at a particular spot in or about the rotor.

DISCUSSION

In this discussion, no attempt will be made to discuss in detail the available references listed in table I. Instead, some representative results of a few of the references will be touched upon in order to illustrate the state of knowledge of the rotor inflow field.

Hovering

The hovering condition has been rather well explored, both experimentally and theoretically. Flow-visualization tests indicate that, above the rotor, the incoming air that is drawn toward the rotor has horizontal as well as vertical components and becomes part of a primarily vertical slipstream only after passing through the rotor. If the rotor is operating outside of the ground-effect region, the slipstream contracts and reaches its maximum velocity well within 1 radius below the rotor plane. In the outer few percent of the blade radius (or "tip loss" region), there is no well-defined slipstream above or below the rotor. Instead, there is a series of small vortices starting at the blade tip and continuing below the rotor that serve as a boundary between the slipstream beneath the rotor and the air outside of it.

In addition to flow-visualization studies, information exists as to the magnitude of the induced-velocity distribution across the rotor disk in hovering. The results of one such study (ref. 3) are shown in figure 1, which compares the induced velocity, as measured in flight, with that estimated by blade-element—momentum theory (ref. 1). Except for the tip-loss region, the agreement is seen to be quite good. Actually, the good agreement as to magnitude and distribution between theory and experiment should be regarded as a fortunate occurrence wherein very simple concepts give reasonable overall answers to a problem which in reality involves a complex flow state. Although similar data are lacking in vertical climb, it is expected that the theory should be as good as it is in hovering.

Vertical Ascent and Descent

The available information regarding the vertical-flight region is summarized in figure 2, which shows the variation in rotor induced velocity with climb and descent velocity, all velocities being made nondimensional by dividing by the induced velocity in hovering. The plot is thus independent of disk loading and air density. The solid parts of the curve show the regions of climb and descent velocity wherein momentum theory (refs. 1 and 8) applies, which, as shown by the representative flow patterns sketched above the curve, are regions wherein a definite slipstream exists through the rotor. At intermediate rates of descent, simple momentum concepts become invalid in that a definite slipstream ceases to exist because of the "canceling" effect of the downward induced velocity by the upward-coming flight velocity. In this intermediate flight region, represented by the dashed curve, it is seen from the sketch that there is a recirculating flow through the rotor in the form of huge vortex rings; hence, the name "vortex ring" region. At large rates of descent, corresponding to power-off flight and beyond, the vortex rings are much smaller and are localized well above the disk.

The dashed curve shown for the vortex-ring state is a composite of flight and wind-tunnel measurements (refs. 6 and 9 to 14). The most important part of this region lies at the lower rates of descent between about 400 and 1,000 ft/min, where it can be seen that the slope of the curve is unstable; that is, the induced velocity increases at a faster rate than does the descent velocity. At fixed pitch, this results in a reduction in thrust with increased descent velocity. This type of instability is a contributing factor toward the well-known troubles that pilots experience when attempting to maintain steady flight in this region (refs. 1 and 15). Tests (ref. 16) have also shown that helicopter tail rotors may also run into this region of instability when the helicopter is experiencing certain rates of yaw.

Low-Speed Forward Flight

Another flight regime in which rotor inflow is the source of various troubles is the transition region in low-speed forward flight. In this region, which extends from about 15 to 30 mph, helicopters typically experience an increase in rotor-blade stress and vibration. The mechanism which gives rise to some of these troubles is not very well understood, but presumably the troubles are due to the fact that the flow changes from a vertical slipstream in hovering to an essentially horizontal flow pattern in forward flight. Certain general aspects of the wake behavior in this speed range are known, however. For example, as the forward speed increases from hovering, the skew angle of the wake increases, the mean value of the induced velocity decreases, and the longitudinal asymmetry of the inflow velocity increases.

The variation of skew angle of the wake with forward speed, as measured on the Langley helicopter test tower (unpublished), is shown in figure 3. As illustrated in the sketch, the skew angle is defined as the angular displacement of the wake from the vertical. It was measured in the region of maximum wake velocity. The data are compared with theory, represented by the solid line in the figure, and it can be seen that the agreement is fairly good.

The variation of the mean value of the induced velocity with forward speed, also obtained on the Langley helicopter test tower (ref. 22), is shown in figure 4. Here, too, both the induced and forward-flight velocities are expressed nondimensionally. The calculated variation, shown by the solid line, serves as a pretty good fairing for the data, except at the upper end of the speed range where the data themselves become questionable. This upper end of the curve corresponds to velocities of about 25 to 30 mph for normal disk loadings.

Some idea of the increase in the asymmetry of the distribution of wake velocity with forward speed is shown in figure 5. The curves represent unpublished test-tower measurements of wake velocity plotted against

nondimensional blade radius in both the forward and rearward parts of the disk, obtained in the vertical plane of symmetry of the rotor and several feet below the disk. The location of the horizontal survey plane of measurements is illustrated on the sketch. It can be seen from the curves that the inflow velocities over the front part of the disk are smaller than those over the rear of the disk, with the mean slope increasing with forward speed. This variation in inflow velocity from front to rear of the disk has been qualitatively known since the days of the early development of rotor theory by Glauert (ref. 18) who showed that its effect on rotor performance was nil. Years later, Seibel (ref. 23), using wind-tunnel gyroplane data, made a quantitative evaluation of the variation and showed how this variation, assumed to be linear, could cause the observed rise in the vibration level of a two-blade helicopter rotor in this region. Theories are available (refs. 18 to 21) that can predict the approximate location and magnitude of the maximum dissymmetry that occurs in the transition region, but the agreement is not precise.

Cruise and High-Speed Forward Flight

At higher speeds, corresponding to the speed for minimum power and beyond, the dissymmetry decreases, as does the magnitude and thus the importance of the induced velocity. Figure 6 (ref. 24) illustrates the variation of the mean inflow angles with forward speed in this higher speed range. The solid curves represent flow angles as measured in flight by a yaw vane located on the tail cone of a helicopter fuselage about 5/8 of a radius behind the center of rotation. As shown on the sketch, flow angles are referenced to the plane perpendicular to the rotor shaft. Measurements were taken at three power conditions and compared with simple momentum theory (assuming uniform inflow), represented by the dashed curve. It can be seen that the theory gives reasonable answers over most of the flight range and can be used, for example, in designing a horizontal tail surface for the helicopter so that it remains effective over a wide range of steady flight conditions.

An insight to the induced-velocity variation across the rotor disk at several speeds above minimum power is available from British flight tests (ref. 26) that used a smoke-visualization technique. A sample of the smoke-flow pictures obtained during the tests is shown in figure 7. The plane of the streamlines is approximately 0.4R on the starboard side and the helicopter was flying at 53 mph. It can be seen that at this speed there is a slight upwash in front of the rotor and then an increasing downwash toward the rear of the disk. The swirls that show up so clearly are due to the main-rotor-blade tips cutting through the streamlines at successive intervals. Induced-velocity magnitudes obtained from photographs such as these can be regarded as only approximate, but the results are still of interest.

An example of the results thus obtained is shown in figure 8, in which the nondimensional induced velocity, measured at three lateral stations on the disk, is plotted against nondimensional radius. Within the scatter of the data, it is seen that the velocity increases toward the rear in an approximately linear fashion over most of the disk. The calculated variation (ref. 21) shown seems to represent fairly well the general idea as to what goes on in regard to the inflow.

In connection with the design and behavior of tandem helicopters, a knowledge of the vertical distribution of downwash some distance behind a rotor is very desirable. An example of such a distribution is available from wind-tunnel tests (ref. 28) and is shown in figure 9. The downwash angle ϵ, expressed in nondimensional form by dividing by the downwash angle at the center line of the rotor $C_T/2\mu^2$ (as calculated by simple momentum theory), is shown as a function of vertical height Z/R above and below the rotor hub for an intermediate tip-speed ratio. The data were obtained at $1\frac{1}{2}$ radii behind the rotor center line at the three-quarter-radius position on the advancing and retreating sides of the disk. Calculated values (ref. 20) are represented by the dashed line and are seen to represent the shape of the measured distribution pretty well.

The interesting point made by these plots is that, as might be expected, the vertical distribution of downwash is nonuniform, with the maximum occurring approximately on a line drawn through the rotor hub and parallel to the flight velocity. The nonuniformity of velocity has explained certain stability and control phenomena that have been observed with a tandem helicopter. The variation in downwash angle experienced by the rear rotor of a tandem helicopter, for example, causes changes in angle-of-attack stability and speed stability with power changes, as well as contributing to a nonlinearity in angle-of-attack stability. Although the data must be considered approximate, it is interesting to note that, for the case shown, the maximum downwash angle reached is almost three times the value that would be calculated at the center of the rotor by simple momentum considerations. Unpublished information from a different series of wind-tunnel tests indicates that the maximum downwash angles measured in survey planes closer to the rotor disk (at the trailing edge of the disk, for example) are about twice the value calculated for the center of the rotor.

CONCLUDING REMARKS

From this brief review of rotor-inflow information, it is quite clear that much work remains to be done, both theoretically and experimentally, before our understanding of rotor inflow can be said to be

thorough. The problems are defined, but the answers are not quantitatively pinned down in all cases. Enough is known about the subject, however, to be extremely useful in calculating and explaining various aspects of rotor behavior.

Langley Aeronautical Laboratory,
National Advisory Committee for Aeronautics,
Langley Field, Va., June 11, 1954.

REFERENCES

1. Gessow, Alfred, and Myers, Garry C., Jr.: Aerodynamics of the Helicopter. The Macmillan Co., c.1952.

2. Carpenter, Paul J., and Fridovich, Bernard: Effect of a Rapid Blade-Pitch Increase on the Thrust and Induced-Velocity Response of a Full-Scale Helicopter Rotor. NACA TN 3044, 1953.

3. Brotherhood, P.: An Investigation in Flight of the Induced Velocity Distribution Under a Helicopter Rotor When Hovering. Rep. No. Aero. 2212, British R.A.E., June 1947.

4. Carpenter, Paul J., and Paulnock, Russell S.: Hovering and Low-Speed Performance and Control Characteristics of an Aerodynamic-Servocontrolled Helicopter Rotor System As Determined on the Langley Helicopter Tower. NACA TN 2086, 1950.

5. Taylor, Marion K.: A Balsa-Dust Technique for Air-Flow Visualization and Its Application to Flow Through Model Helicopter Rotors in Static Thrust. NACA TN 2220, 1950.

6. Meijer Drees, J., and Hendal, W. P.: Airflow Patterns in the Neighbourhood of Helicopter Rotors. Aircraft Engineering, vol. XXIII, no. 266, Apr. 1951, pp. 107-111.

7. Harrington, Robert D.: Full-Scale-Tunnel Investigation of the Static-Thrust Performance of a Coaxial Helicopter Rotor. NACA TN 2318, 1951.

8. Glauert, H.: Notes on the Vortex Theory of Airscrews. R. & M. No. 869, British A.R.C., Dec. 1922.

9. Lock, C. N. H., Bateman, H., and Townend, H. C. H.: An Extension of the Vortex Theory of Airscrews With Applications to Airscrews of Small Pitch, Including Experimental Results. R. & M. No. 1014, British A.R.C., 1926.

10. Glauert, H.: The Analysis of Experimental Results in the Windmill Brake and Vortex Ring States of an Airscrew. R. & M. No. 1026, British A.R.C., Feb. 1926.

11. Castles, Walter, Jr., and Gray, Robin B.: Empirical Relation Between Induced Velocity, Thrust, and Rate of Descent of a Helicopter Rotor As Determined by Wind-Tunnel Tests on Four Model Rotors. NACA TN 2474, 1951.

12. Hafner, Raoul: Rotor Systems and Control Problems in the Helicopter. Aeronautical Conference - London, J. Laurence Pritchard and Joan Bradbrooke, eds., R.A.S., 1948, pp. 579-632.

13. Lock, C. N. H.: Note on the Characteristic Curve for an Airscrew or Helicopter. R. & M. No. 2673, British A.R.C., June 1947.

14. Brotherhood, P.: Flow Through Helicopter Rotor in Vertical Descent. R. & M. No. 2735, British A.R.C., July 1949.

15. Stewart, Wm.: Helicopter Behaviour in the Vortex Ring Conditions. C. P. No. 99, British A.R.C., Nov. 1951.

16. Amer, Kenneth B., and Gessow, Alfred: Charts for Estimating Tail-Rotor Contribution to Helicopter Directional Stability and Control in Low-Speed Flight. NACA TN 3156, 1954.

17. Meijer Drees, J.: A Theory of Airflow Through Rotors and Its Application to Some Helicopter Problems. Jour. Helicopter Assoc. of Great Britain, vol. 3, no. 2, July-Aug.-Sept. 1949, pp. 79-104.

18. Glauert, H.: A General Theory of the Autogiro. R. & M. No. 1111, British A.R.C., 1926.

19. Coleman, Robert P., Feingold, Arnold M., and Stempin, Carl W.: Evaluation of the Induced-Velocity Field of an Idealized Helicopter Rotor. NACA WR L-126, 1945. (Formerly NACA ARR L5E10.)

20. Mangler, K. W.: Calculation of the Induced Velocity Field of a Rotor. Rep. No. Aero. 2247, British R.A.E., Feb. 1948.

21. Castles, Walter, Jr., and De Leeuw, Jacob Henri: The Normal Component of the Induced Velocity in the Vicinity of a Lifting Rotor and Some Examples of Its Application. NACA TN 2912, 1953.

22. Carpenter, Paul J.: Effect of Wind Velocity on Performance of Helicopter Rotors As Investigated With the Langley Helicopter Apparatus. NACA TN 1698, 1948.

23. Seibel, Charles: Periodic Aerodynamic Forces on Rotors in Forward Flight. Jour. Aero. Sci., vol. 11, no. 4, Oct. 1944, pp. 339-342.

24. Gustafson, F. B.: Desirable Longitudinal Flying Qualities for Helicopters and Means To Achieve Them. Aero. Eng. Rev., vol. 10, no. 6, June 1951, pp. 27-33.

25. Oliver, A. L.: The Low Speed Performance of a Helicopter. C. P. No. 122, British A.R.C., May 1952.

26. Brotherhood, P., and Stewart, W.: An Experimental Investigation of the Flow Through a Helicopter Rotor in Forward Flight. R. & M. No. 2734, British A.R.C., Sept. 1949.

27. Wheatley, John B., and Hood, Manley J.: Full-Scale Wind-Tunnel Tests of a PCA-2 Autogiro Rotor. NACA Rep. 515, 1935.

28. Fail, R. A., and Eyre, R. C. W.: Downwash Measurements Behind a 12-Ft Diameter Helicopter Rotor in the 24-Ft Wind Tunnel. R. & M. No. 2810, British A.R.C., Sept. 1949.

TABLE I

SUMMARY OF ROTOR-INDUCED-FLOW INFORMATION

Type of information	Source	Reference	Remarks
Hovering			
Theory	Blade-element—momentum	1, 2	Magnitude and distribution
Measurements and smoke flow	Flight tests	3	Magnitude and distribution
Measurements	Test tower	2, 4, unpublished	Magnitude and distribution
Balsa dust and smoke flow	Small scale (single and coaxial)	5, 6	Distribution
Applications	Performance calculations	1, 7	Single and coaxial
Vertical ascent and descent			
Theory	Momentum	1, 8	Mean value
Measurements and smoke flow	Small and large scale	6, 9, 10, 11, 12, 13	Magnitude and distribution
Smoke flow	Flight tests	14	Distribution
Applications	Performance	1	
	Stability and control	15, 16, 17	
Low-speed forward flight			
Theory	Vortex	18, 19, 20, 21	
Measurements	Test tower	4, 22, unpublished	Magnitude and distribution and flow angles
	Indirect	23	
Applications	Stability and control	17, 24	
	Vibrations	17, 23	
	Performance	17, 22, 25	
Cruise and high-speed forward flight			
Theory	Momentum and vortex	17, 18, 19, 20, 21	
Smoke flow	Small-scale and flight tests	6, 26	Flow angles and distribution
Measurements	Large-scale wind tunnel	27, 28	Magnitude and distribution
	Flight tests	24	Flow angles
Applications	Stability and control	24	
	Performance	1	

INDUCED-VELOCITY DISTRIBUTION IN HOVERING

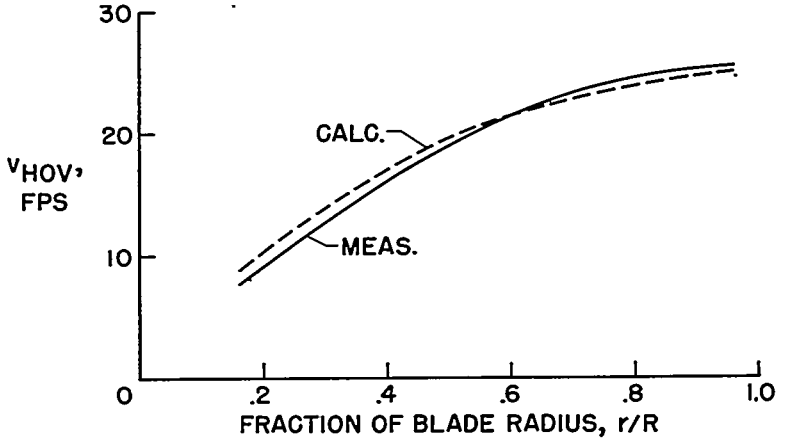

Figure 1

INDUCED-VELOCITY RELATIONS IN VERTICAL FLIGHT

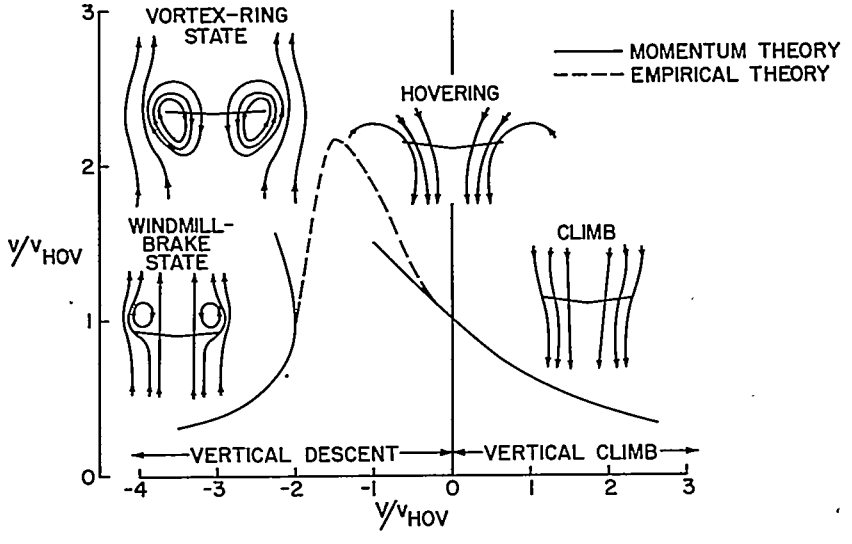

Figure 2

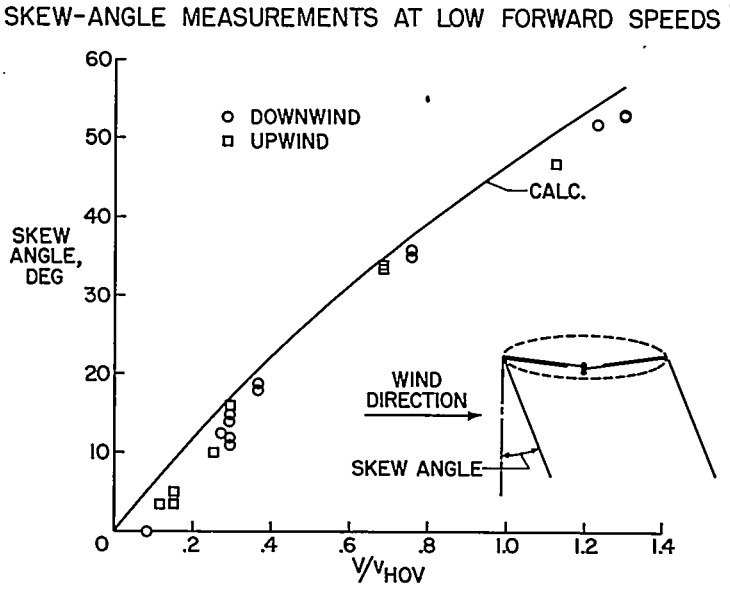

Figure 3

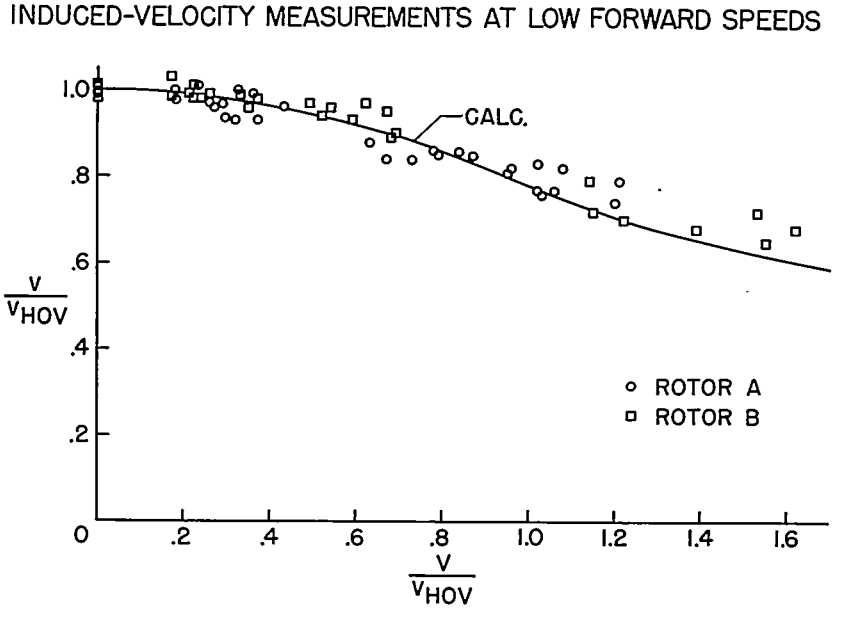

Figure 4

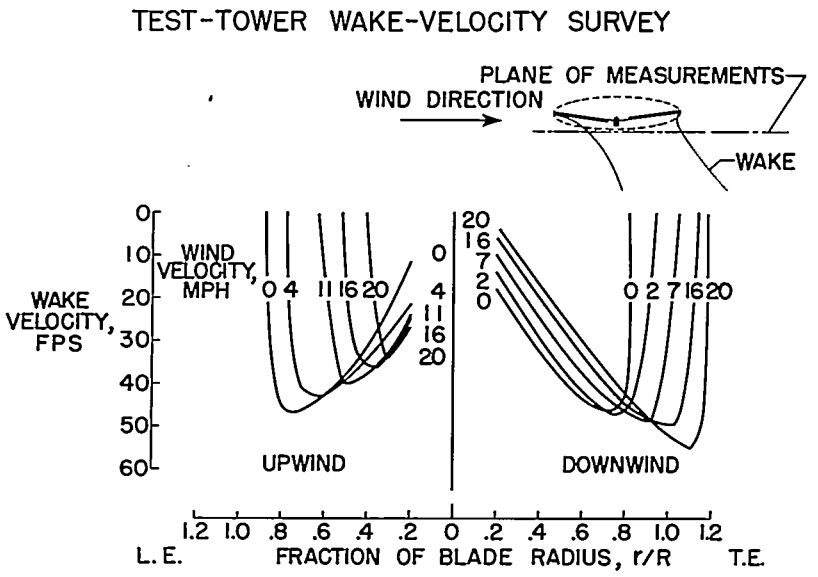

Figure 5

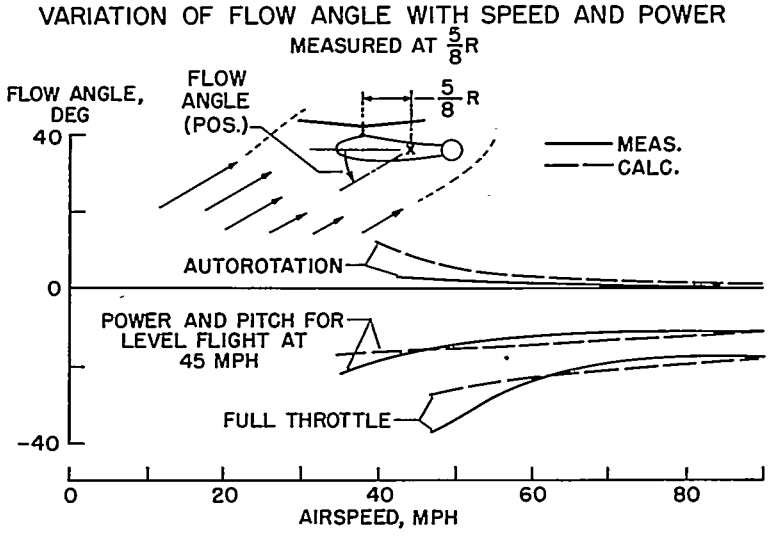

Figure 6

SMOKE FLOW TESTS IN FORWARD FLIGHT
V= 53 MPH

Figure 7

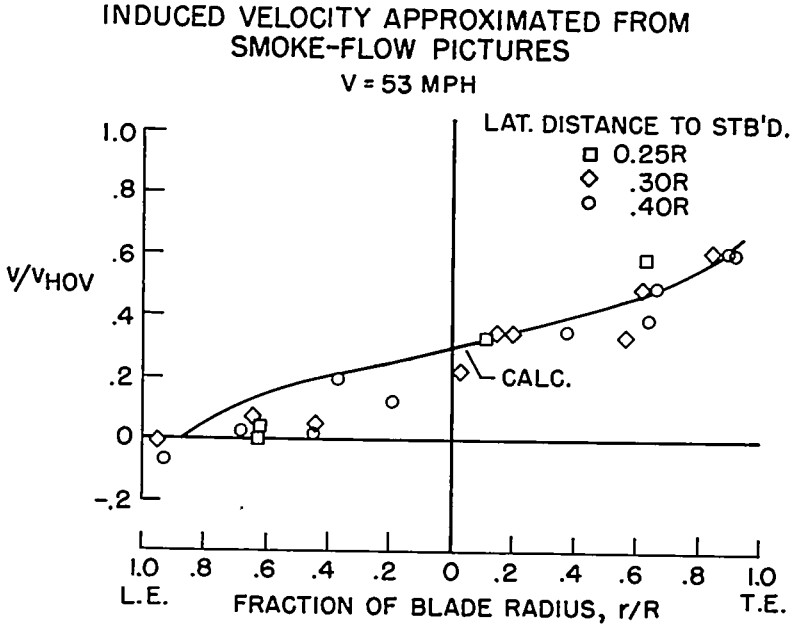

Figure 8

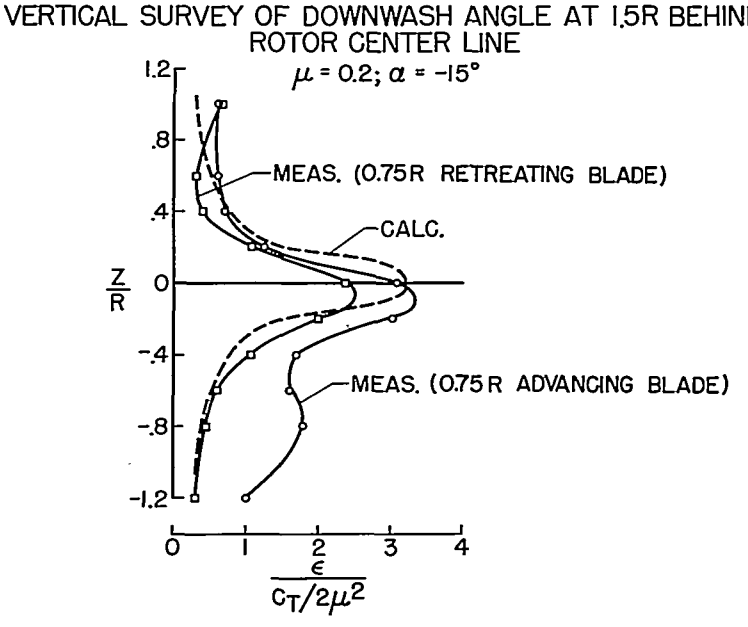

Figure 9

NACA-Langley - 8-13-54 - 1000